



“Structural Behavior of Corroded R.C. Beams Contained Nano-Silica”

Ahmed Ibrahim Marawan ¹, Ahmed Saeed Debaiky ², Ahmed Hassan Abd El-Kareem²

¹ *Department of Civil Engineering, Faculty of Engineering, Delta University, Gamsa, Egypt.*

² *Department of Civil Engineering, Faculty of Engineering, Banha University, Banha, Egypt.*

ABSTRACT

Reinforced concrete structures are considered permanent structures. But reinforced concrete is considered a composite material where reinforcement is embedded in concrete to act as one unit. One of the issues that threatens the area of steel and the bond between concrete and reinforcement is corrosion, especially in marine environments. In marine structures, one of the most attacking materials is chlorides, which cause corrosion. The good quality of concrete has an effective influence on reducing corrosion. In this paper, 9- specimens were fabricated to evaluate the effects of the addition of Nano-Silica on the structural behavior of corroded R.C. beams. 5 concrete mixes with different ratios of Nano-Silica (0%, 1%, 1.5%, and 2% as a replacement for cement weight) were used to cast the specimens. Specimens were divided into 2 groups. Group A consisted of 4-beams that were corroded by a constant electrical current density. Also, Group B consisted of 5-beams, which were corroded by wetting and drying cycles of salty solution. The experimental results included the compressive strength of concrete, steel mass loss, ultimate capacity load, and load deflection behavior. Finally, it was noticed that Nano-Silica improved the structural properties of corroded beams.

Keywords: Corrosion, Nano-Silica, Beam retrofitting.

1. Introduction

Reinforced concrete is one of the most widely used construction materials in the world today. Reinforced concrete is a composite material wherein reinforcement is embedded in the concrete and behaves as a single structural unit depending on the bonding between both the concrete and the rebar. This provides the known mechanical properties and high durability along with their serviceability life. In modern construction practice, many failures have happened according to the serviceability limit state when compared with failures according to the ultimate limit state, so the durability limit state is clearly defined in new construction practices. One of the concerns of durability is steel corrosion, which has become one of the major issues discussed in the construction field, particularly in corrosive environments [1, 2].

Metal corrosion is primarily caused by their electrochemical stability, where they tend to be more stable compounds (oxides or hydroxides) [3]. Steel corrosion in concrete is complicated because the concrete mixture's high alkalinity protects the cohesive oxide thin film around the bar. When corrosion is initiated, steel bars dissolve into the surrounding area as the passive film is degraded locally. The depassivated regions expand due to an increase in the volume of corrosion products. When the corrosion products become solid, they have a larger volume than the original volume of the metal, which results in high pressure around the embedded steel bars. As a result, the concrete cover expands, potentially causing cracking, spalling, and delamination of the concrete structure [4-8]. In addition, the corrosion process has multiple interconnected effects, including a reduction in the cross-sectional area of the steel bars due to the formation of corrosion products and the degradation of the steel-concrete bond. The severity of reinforcement corrosion impacts the performance of RC structures, including adverse effects on flexural strength, ductility, bond behavior, and failure mode. These phenomena compromise the structural integrity of RC structures and may cause them to fail prematurely [9-12].

Reinforcement corrosion is a gradual process in natural conditions that depends on several factors, such as moisture, humidity, oxygen, aggressive conditions, concrete quality, and fiber reinforcement content [3, 4]. To break the corrosion cycle, high compressive strength concrete with low porosity must be used. There are numerous methods for producing dense concrete with high compressive strength and low porosity, including Nano-concrete. Nanoscience technology is a recent field in materials science and engineering. Nanoparticles are the most important products of nanotechnology [5]. In the field of concrete technology, nanoparticles are

used to increase the durability and strength of concrete [6]. Among the nanoparticles, nano-silica has attracted the attention of several researchers because it has excellent pozzolanic activity in cement-based materials [7]. Some researchers have studied the effects of nano-SiO₂ particles on the performance of cement-based materials such as mortar, cement paste, and concrete [8]. Nano-silica particles improve the mechanical properties and durability characteristics of cement-based materials by enhancing the density of the binding matrix and improving the interfacial transition zone (ITZ) between aggregates and the cement paste [9]. Du et al. [10] studied the durability properties of concrete containing nano-silica at small dosages of 0.3 % and 0.9 %, respectively. The use of low dosages of nano-silica results in a combined contribution of the nanofiller effect and the pozzolanic reaction. This means that the beneficial effects of nano-silica can be obtained with lower dosages of nanoparticles [11]. If more than 5 % of nano-silica replaces cement, it may have adverse effects on the durability and mechanical characteristics of concrete [8].

Prasath et al. [12] tested the mechanical properties of the designed mixes, such as durability, compressive strength, and flexural strength. The mixes were varied in content of silica-fume (5%, 7.5%, 10%, and 12.5%) and content of Nano-Silica (1%, 2%, 3%, and 4%) as cement replacement. It was found that the mix of 7.5% silica-fume and 2% Nano-Silica has perfect properties. Finally, R.C. specimens were fabricated and corroded. Non-corroded concrete specimens had the lowest mass loss of steel. Zapata et al. [13] examined the mixing of Nano-Silica with Micro-Silica. They founded an improvement in the mechanical properties of concrete where the highest strength, lowest water absorption, and lowest chloride penetration were achieved in Micro/Nano concrete. Arunbalaji et al. [14] performed an experimental study on the behaviour of reinforced concrete R.C. beams containing Micro-silica (10%) and NS (0%, 0.5%, 1.0% or 1.5%). The concrete mixes had a fixed water/binder ratio of 0.53. The development of mechanical strength indicated that a cement replacement of 10% Micro-silica and 0.5% NS was the optimal proportion. A similar study was carried out by Hanadi [15] to investigate the shear behaviour, cracking, and ultimate shear capacities of beams made from NS-dosed reactive powder concrete. The research covered four parts. The first part dealt with an experimental study of the effects of varying some material parameters on the mechanical properties of the concrete. One of these material parameters was NS content (0%, 1.0%, 2.0% or 3.0%). It was found that increasing the NS content from 0 to 3.0% led to an increase in the diagonal cracking and ultimate shear strengths by 35.7% and 25.1%, respectively.

To corrode any R.C. element under natural conditions to a significant level of corrosion will take many years. Therefore, many researchers developed different techniques to accelerate the corrosion process. There are two types of accelerated corrosion: naturally accelerated corrosion and forced accelerated corrosion.

Galvanostatic corrosion is the technique most commonly used in laboratories to accelerate corrosion in test specimens [16]. In this method, constant-intensity direct current is used where the positive terminal is connected to the reinforcing bars. The reinforcing bars acted as an anode. On the other hand, the negative terminal is connected to the cathode. The cathode can be represented by a black steel bar or a stainless-steel bar that can be embedded in the concrete element, or by a wire mesh or plate that can be placed externally underneath the specimens. The wet concrete body acts as an electrolyte, providing an electrical connection between the anode and cathode. Alonso and Andrade [17] concluded that the value of current density (total current/total steel surface area) according to natural steel corrosion is between 0.1 to 10 $\mu\text{A}/\text{cm}^2$. The researchers used this concept to speed up the corrosion process by increasing current density. El-Maaddawy and Soudki [18] reported that the impressed current density of less than 200 $\mu\text{A}/\text{cm}^2$ causes structural deterioration that would be observed as natural corrosion.

For naturally accelerated corrosion, cycles of wetting and drying with the contribution of chloride ions in the form of salt solution were used to accelerate the corrosion process. The corrosion created by this process is similar to the corrosion that occurs in splash zones in coastal structures where R.C. structures are exposed to tidal waves or splashing by sea water. Some researchers mix chlorides with concrete mixes to accelerate the corrosion of R.C. structures by chloride attack (sea water). The range of the mixed chlorides ranges from 1% to 5% by weight of cement, as reported by Mangat and EL-Graf [19] and El-Maaddawy and Soudki [28] respectively. Other researchers immersed their specimens in a 3.5% NaCl solution. The selected chloride concentration was chosen to simulate the chloride concentration in sea water [20].

2. Objectives

The objective of this study is to evaluate the influence of adding Nano-Silica on the structural behavior of corroded beams. The compressive strength of concrete, steel mass loss, load carrying capacity, and load deflection curves were the parameters of the results of the study.

3. Experimental Program

9-R.C. beams were divided into two groups (A and B). Group A consisted of 4 beams, while Group B consisted of 5 beams. Beams in each group were cast with variable ratios of Nano-Silica. The variation between the two groups was the method of accelerated corrosion, where group A was corroded by the forced accelerated corrosion method and group B was corroded by the naturally accelerated corrosion method. Table (1) summarizes experimental program.

Table (1): Summary of experimental program

Specimens	Group	Accelerated corrosion method	Micro-Silica (%)	Nano-Silica (%)
AFC	A	F	0	0
AFMS8			8	0
AFMNS81			8	1
AFMNS81.5			8	1.5
BNC	B	N	0	0
BNMS8			8	0
BNMNS81			8	1
BNMNS81.5			8	1.5
BNMNS82			8	2

F: Forced accelerated corrosion method N: Naturally accelerated corrosion method
 MS: Specimen contained Micro-silica as a replacement of cement
 MNS: Specimen contained Micro-silica and Nano-silica as a replacement of cement

3.1. Details of specimens

A total of nine specimens were fabricated to study all the variable parameters that affected the behavior of corroded R.C. beams. The specimens were divided into two groups: Group A consisted of 4-R.C. beams. The dimensions of the specimens were 1510 mm long, with a cross section of 110 mm in width and 210 mm in thickness. Each specimen had two 12-mm diameter deformed bars that were placed longitudinally in the tension zone. Also, two 6-mm diameter plain bars were placed longitudinally in the compression zone. As shear reinforcement, 6 mm diameter stirrups were used with 100 mm spacing. The clear concrete cover was kept at 20 mm. In this group, flexural steel bars were bent at the ends of the beams and extended approximately 50 mm over the top surface of the specimens to facilitate electrical current connection. Figure (1) illustrates all the details of the specimens. Group B consisted of 10-R.C. beams. The dimensions of the specimens were 1810 mm long, with a cross section of 110 mm width and 210 mm thickness. Each specimen had two 12 mm diameter deformed bars that were placed longitudinally in the tension zone. Also, two 6 mm diameter plain bars were placed longitudinally in the compression zone. As shear reinforcement, 6 mm diameter stirrups were used with 100 mm spacing. The clear concrete cover was kept at 20 mm. Figure (2) illustrates all the details of the specimens.

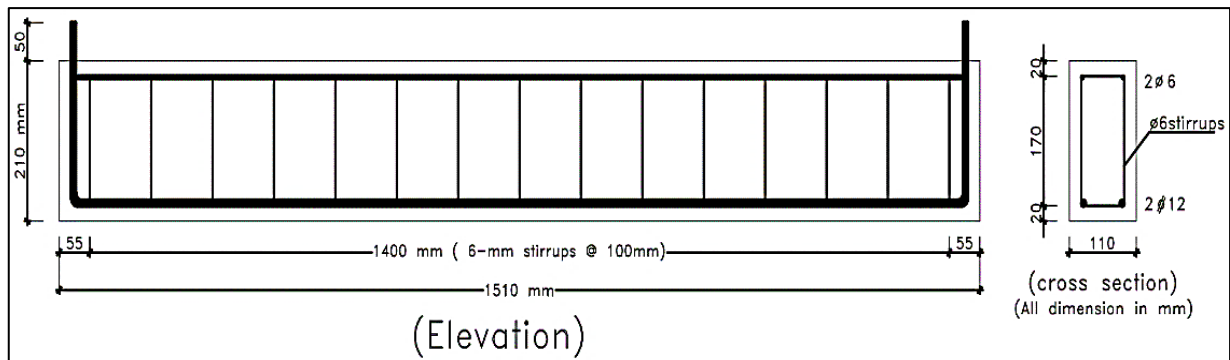
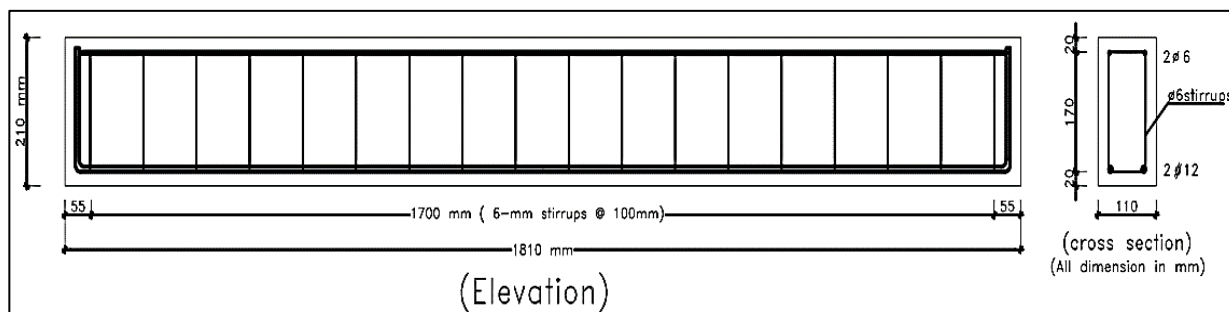


Figure (1): Details of specimens in group A

Figure (2): Details of specimens in group B

3.2 Materials properties

For coarse aggregates, crushed graded dolomite, which had a 10 mm maximum size and a 2.66 specific gravity, was used. For fine aggregates, natural siliceous sand, which had a specific gravity of 2.7, was used. From visual examination, the sand was free from silt, clay, impurities, and organic materials. Ordinary Portland cement has a grade of 52.5 N and was used for tests. Ordinary clean water, free from any suspended particles or chemical substances, was used for both mixing and curing. Locally, Nano-Silica, which is considered a highly pozzolanic material, was used. Transmission Electronic Microscopic (TEM) of Nano-silica was performed as shown in Figure (3). The Micro-Silica (silica-fume) and superplasticizer (Glenium C35) were



obtained from BASF Company. Two 12 mm diameter deformed bars were used as bottom steel. 12 mm bars were high tensile steel with a yield stress of about 617 MPa and an ultimate stress of 730 MPa. Also, two 6 mm diameter plain bars were used as top steel and stirrups. 6 mm bars were high tensile steel with a yield stress of about 254 MPa and an ultimate stress of 365 MPa.

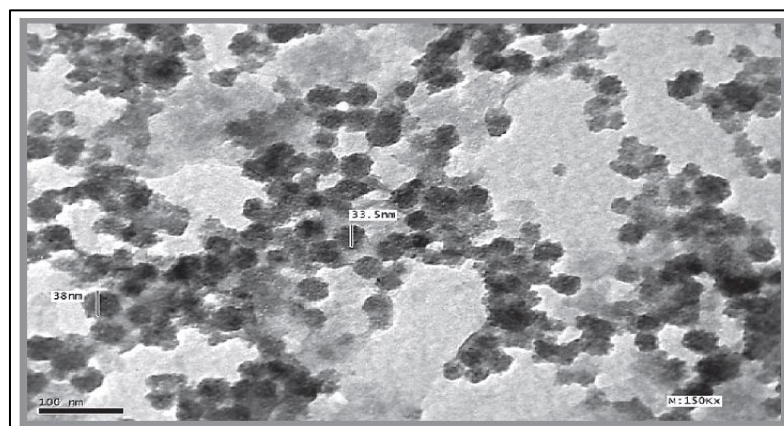


Figure (3): TEM of Nano-Silica particles

3.3. Concrete mixes design

5 concrete mixes were used for casting for all specimens where proportions of concrete mixes were given in Table (2). All mixes had a constant water to cementitious material (W/C) ratio of 0.43 with a total cementitious material content of 400 kg/m³. Cementitious materials were cement, Micro silica and Nano-silica. Therefore, portions of Micro-Silica and Nano-Silica were added as replacements for cement weight. The first mix (CO) was used as a control mix. The second mix (MS8) was conducted by adding micro-silica (8.0% of the cement weight as replacement). The other three mixes were formed by adding different ratios of Nano-silica of 1%, 1.5%, and 2% of the cement weight as replacement, respectively.

Concrete Mix Notation	Coarse Aggregate	Fine Aggregate	Cement	Water	S. P *	Micro Silica	Nano Silica
-----------------------	------------------	----------------	--------	-------	--------	--------------	-------------

Table (2):

Co	1200	600	400	172	0	0	0
MS8	1200	600	368	172	8	32	0
MNS81	1200	600	364	172	8	32	4
MNS81.5	1200	600	362	172	8	32	6
MNS82	1200	600	360	172	8	32	8

Concrete mixes proportions (K)

*S. P: Superplasticizer

3.4. Accelerated corrosion setup

The accelerated corrosion method was one of the techniques to accelerate corrosion in structural elements by applying an electrical current using an electrolyte solution or applying cycles of wetting and drying with a salt solution. Two different methods of the accelerated corrosion process were used to corrode all the specimens. 4-specimens in group A were corroded by the forced accelerated corrosion method. On the other hand, 5-specimens in group B were corroded by using the naturally accelerated corrosion method.

Forced accelerated corrosion: To speed up the corrosion process, $400\mu\text{A}/\text{cm}^2$ electrical current density was impressed through steel bars for 18 days. Also, a NaCl solution was used. The corrosion cell consists of **(I) an anode**, which was represented by steel bars, **(II) a cathode**, which was represented by steel wire mesh, and **(III) an electrolyte solution**, which was formed by 3.5 % NaCl solution. A steel-wire mesh was wrapped around the beam's body. The anode was connected to the positive terminal of the power supply. On the other hand, the cathode was connected to the negative terminal. Between the beam body and the steel wire mesh was a gunny sack piece. The NaCl solution had been sprayed on the beams two times a day (once around 7 a.m. and again around 2 p.m.). Figure (4) gives a clear show for corrosion cell contents. The value of the electrical current density and time of the corrosion process were determined according to the required steel mass loss. The required mass loss was 8% of steel weight. The required amount of steel mass loss was calculated by Faraday's law as the following equation:

$$\Delta m = \frac{M \cdot I \cdot t}{Z \cdot F} \quad \text{Eq. (1)}$$

Where:

Δm : Required amount of steel mass loss

I: Electrical current (Amperes)

Z: the ionic charge (2 for steel)

M: Atomic weight of steel (56 g)

t: Time of corrosion process (second)

F: Faraday's constant (96500 Amperes. Second)

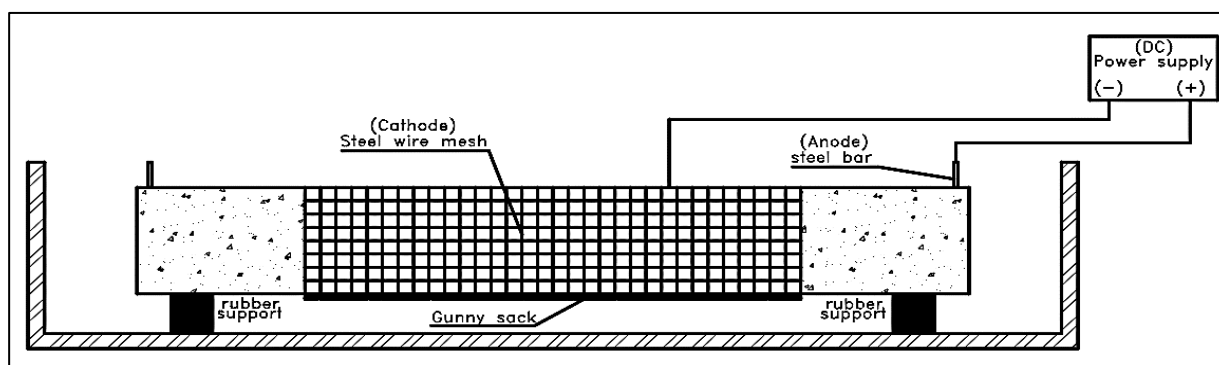


Figure (4): Forced accelerated corrosion cell

Naturally accelerated corrosion: Beams were corroded by an aggressive environment of salty solution, humidity, and temperature. The specimens were placed in tank where they were exposed to weather conditions of humidity and temperature. The specimens were left to corrode for 500 days before being tested. During this period, wetting and drying cycles were used to accelerate the corrosion process. 3.5% NaCl was sprayed every day at 7 AM and 2 PM in the wet half cycle. The weather was used to dry the specimens in a

half-dry cycle. This duration is equivalent to many years of field exposure to natural weather. The summer weather provided the high temperature and humidity needed to expedite the corrosion process.

3.5. Testing setup and procedure

All specimens were tested in testing frame of reinforced concrete research laboratory of faculty of engineering, Banha University as shown in Figure (5). The load was applied by a hydraulic jack that was connected to a braced frame. To measure the acting load, a load cell was connected to a jack. The load was acted at central point of beam. The supports were placed 100 mm from each end of the beam. 3 LVDT were used to measure the deflection accompanied to load as shown in Figure (6).



Figure (5): Frame used in testing

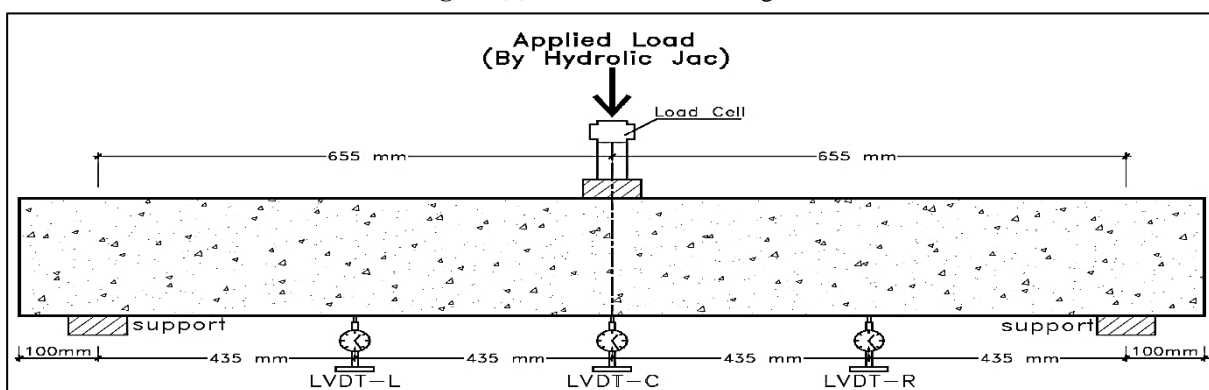


Figure (6): Test setup and procedure

4. Experimental Program

4.1. Compressive strength

12-cubes were tested after 28 days to determine the compressive strength for beams in group A (beams were corroded by a forced accelerated corrosion process). The other 15-cubes were tested after 500 days to determine the compressive strength for beams in group B (beams were corroded by a naturally accelerated corrosion process). All the cubes were cured under the same conditions as the beams.

For the concrete strength of concrete mixes after 28 days, Figure (7) shows the compressive strength of 4 concrete mixes (CO, MS8, MNS81, and MNS81.5). Control mix (CO) had the lowest compressive strength of 50.7 MPa, whilst MS8, MNS81, and MNS81.5 had compressive strengths of 54 MPa, 62.6 MPa, and 58.1 MPa, respectively. The increases in compressive strength of MS8, MNS81, and MNS81.5 were 7%, 24%, and 15% respectively.

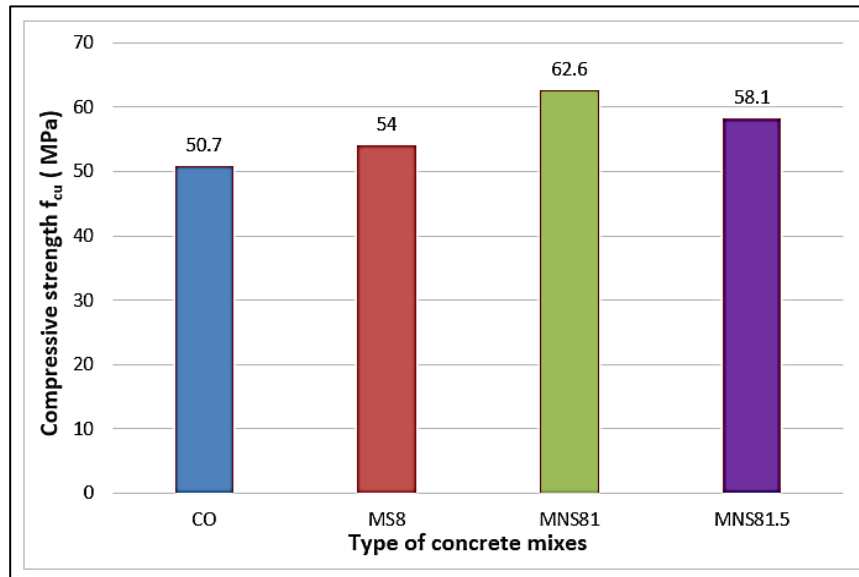


Figure (7): Compressive strength after 28-days

For the concrete strength of concrete mixes after 500 days, Figure (8) shows the compressive strength of 5 concrete mixes (CO, MS8, MNS81, MNS81.5, and MNS82). Control mix (CO) had the lowest compressive strength of 41 MPa, whilst MS8, MNS81, MNS81.5 and MNS82 had compressive strengths of 46.4 MPa, 59.6 MPa, 54.3 MPa and 52.5, MPa respectively. The increases in compressive strength of MS8, MNS81, MNS81.5, and MNS82 were 13%, 45%, 32%, and 28%, respectively.

Also, from comparing the compressive strength of concrete mixes after 28-days and 500-days, there was a decrease in the compressive strength at 500-days due to the penetration of chloride ions of the long-immersed specimens. This shows the negative effect of chlorides on compressive strength over the long term [21]. The decrease in compressive strength of the CO mix was 19.1%. Also, the decrease in compressive strength of the MS8 mix was 14.1%. In addition, the decrease in compressive strength of the MNS81 mix was 4.8%. Finally, the decrease in compressive strength of the MNS81.5 mix was 6.5%.

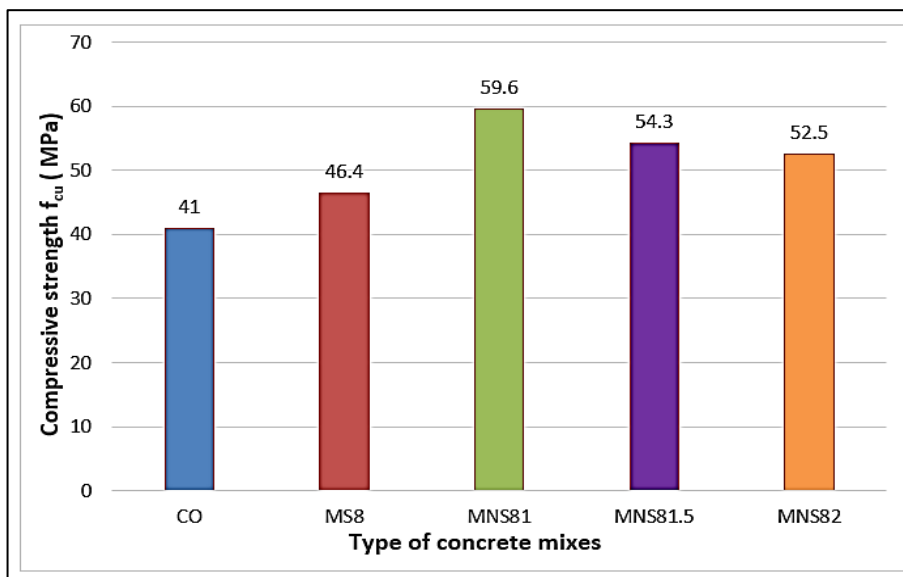


Figure (8): Compressive strength after 500-days

4.2. Steel mass loss

After end of forced corrosion process and also after experimental tests. The steel bars were extracted from beams from beams in group A then cleaned from rust. The steel mass loss was calculated according to the following equation:

$$\% \text{ of mass loss} = \frac{(\text{Initial Weight} - \text{Final Weight})}{\text{Initial Weight}} \times 100 \quad \text{Eq. (2)}$$

The control beam (AFC) had the highest mass loss of steel, while the other beams AFMS8, AFMNS81, and AFMNS81.5 had the lowest mass loss. As shown in Figure (9), the average percentage of mass loss of beams AFC, AFMS8, AFMNS81, and AFMNS81.5 was 6.5, 5, 4.2, and 4.8 respectively.

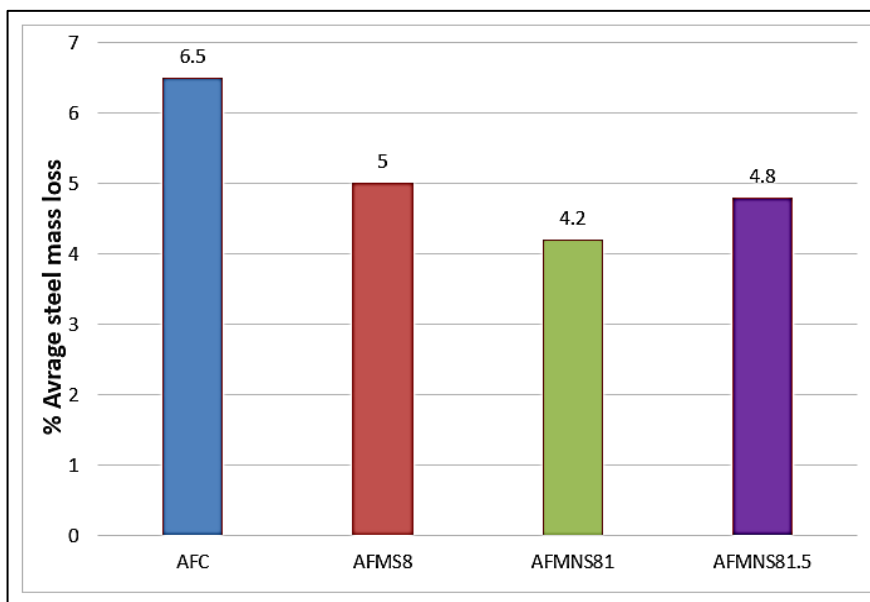


Figure (9): Steel mass loss of forced corroded beams

4.3. Ultimate load

Figure (10) shows the ultimate load capacity for beams in group A. It is clear that the beams with Nano-Silica had the maximum ultimate load. The peak loads for beams AFC, AFMS8, AFMNS81 and AFMNS81.5 were 75.6 kN, 78.5 kN, 86.9 kN and 80.2 kN, respectively. The beam with 1% Nano-silica, the beam with 1.5% Nano-silica and the beam with 8% Micro-silica only had an average increase in ultimate load capacity of 15%, 6% and 4%, respectively when they were compared with the control beams.

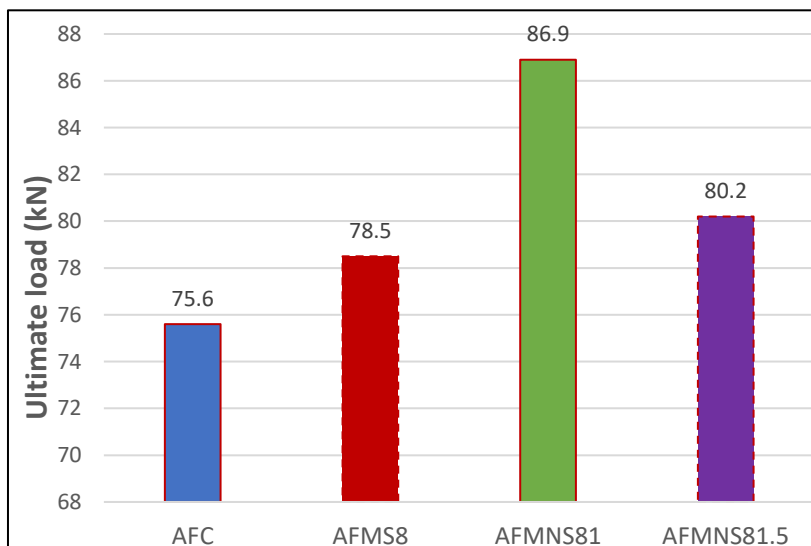


Figure (10): Ultimate load capacity for beams in group A

Figure (11) shows the ultimate load capacity for beams in group B. It is clear that the beams with Nano-Silica had the maximum ultimate load. The peak loads for beams BNC, BNMS8, BNMNS81, BNMNS81.5 and BNMNS82 were 59.3 kN, 62.1 kN, 69.4 kN, 67.5 kN and 65 kN, respectively. The beam with 1% Nano-silica, the beam with 1.5% Nano-silica, the beam with 2% Nano-silica and the beam with 8% Micro-silica only had an average increase in ultimate load capacity of 17%, 13%, 10% and 5%, respectively when they were compared to with control beam.

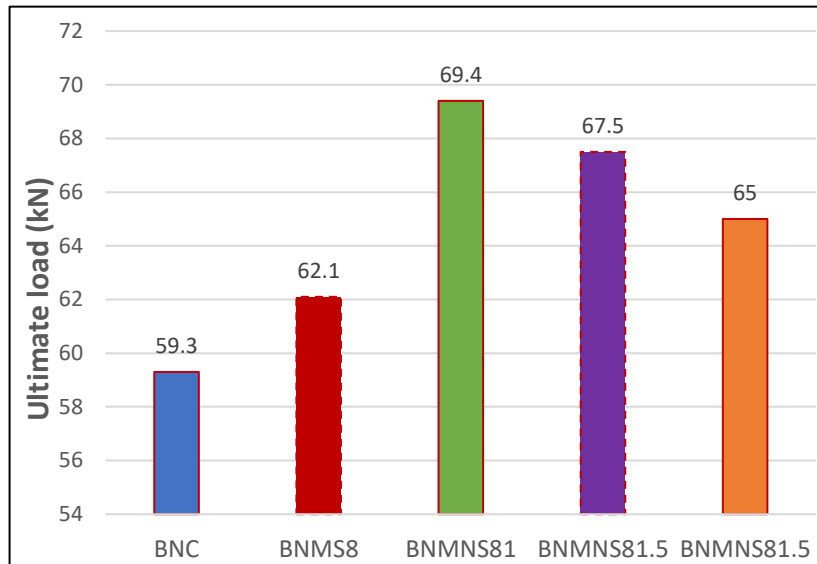


Figure (11): Ultimate load capacity for beams in group B

4.4. Load deflection curves

For beams in group A, Figure (12) shows the load deflection curves. The beam AFC failed at 75.6 kN with a mid-span deflection of 15.1 mm. Also, the beam AFMS8 failed at 78.5 kN with a mid-span deflection of 13.3 mm. In addition, the beam AFMNS81 failed at 86.9 kN with a mid-span deflection of 15.7 mm. Finally, the beam AFMNS81.5 failed at 80.3 kN with a mid-span deflection of 14 mm.

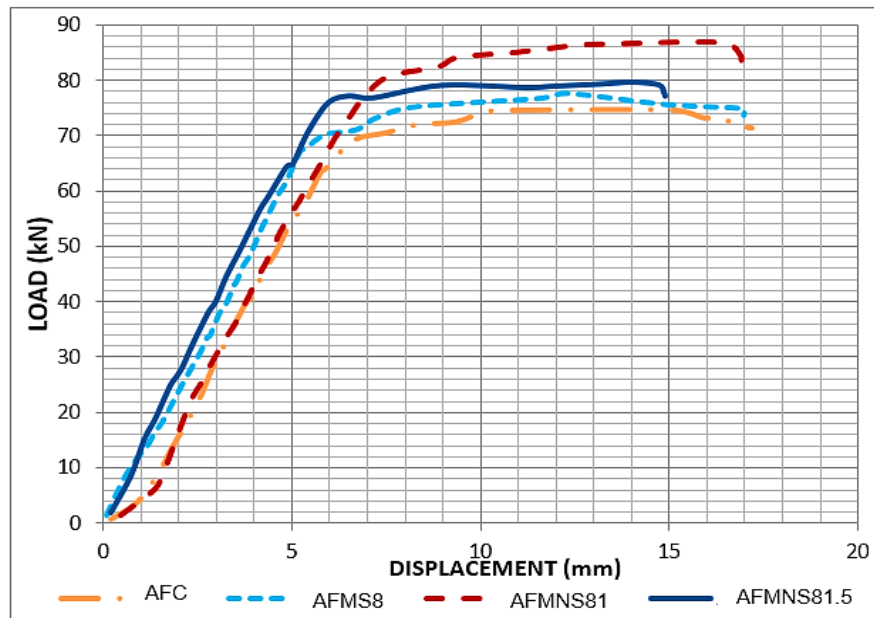


Figure (12): Ultimate load capacity for beams in group A

For beams in group B, Figure (13) shows the load deflection curves. The beam BNC failed at 59.3 kN with a mid-span deflection of 11.8 mm. Also, the beam BNMS8 failed at 62.1 kN with a mid-span deflection of 24.5 mm. In addition, the beam BNMNS81 failed at 69.4 kN with a mid-span deflection of 29.2 mm. Moreover, the beam BNMNS81.5 failed at 67.4 kN with a mid-span deflection of 31.4 mm. Finally, the beam BNMNS82 failed at 65 kN with a mid-span deflection of 36 mm.

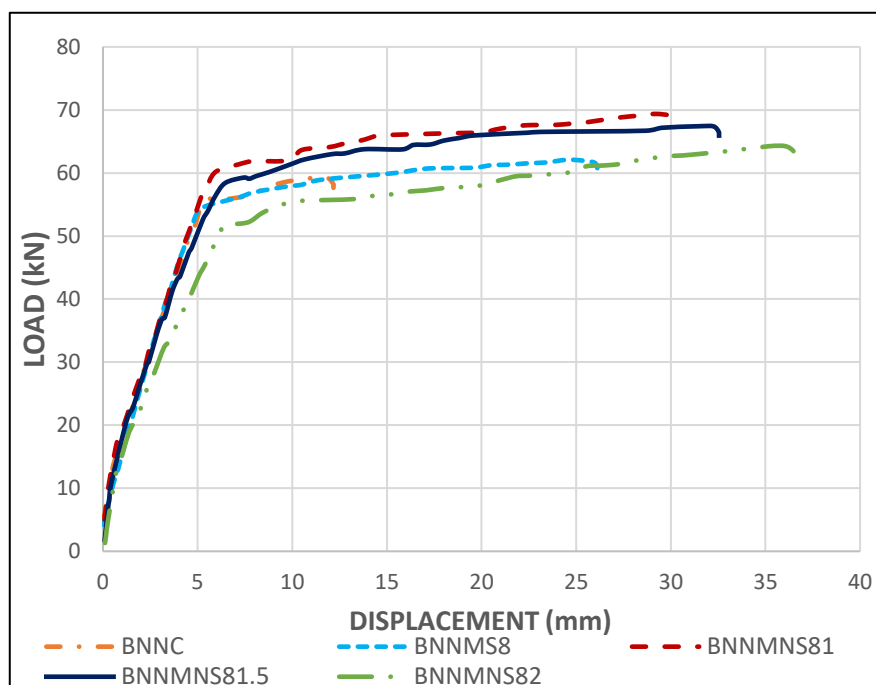


Figure (13): Ultimate load capacity for beams in group B

Conclusion

Based on the investigation and experimental results, which were described, a number of conclusions may be considered for addition of nano-silica. The findings are summarized below:

- From the results, adding Nano-Silica had a significant influence on the behavior of corroded R.C. beams. Compressive strength, steel mass loss, ultimate load capacity, and load-deflection were improved.
- The Nano concrete mixes (MNS81 and MNS81.5) after 28 days of corrosion had a compressive strength of 62.6 MPa and 58.1 MPa, respectively. Although the control mix (CO) had 50.7 MPa. The increases in compressive strength of MNS81 and MNS81.5 were 24% and 15%, respectively.
- The Nano concrete mixes (MNS81, MNS81.5, and MNS82) after 500 days of corrosion had a compressive strength of 59.6 MPa, 54.3 MPa, and 52.5 MPa, respectively. The control mix (CO) on the other hand had 41 MPa. The increases in compressive strength of MNS81, MNS81.5 and MNS82 were 45%, 32%, and 28%, respectively.
- Due to chloride penetration, the compressive strength of concrete decreased after 500 days of corrosion. But Nano concrete mixes showed the lowest decrease in compressive strength. The decrease in compressive strength of CO mix, MNS81 mix, and MNS81.5 mix was 19.1%, 4.8%, and 6.5%, respectively.
- For steel mass loss, the Nano concrete beams (AFMNS81 and AFMNS81.5) had the lowest steel mass loss. The average percentage of mass loss of concrete beams AFC, AFMNS81, and AFMNS81.5 was 6.5, 4.2, and 4.8 respectively.
- The beams, which contained Nano-Silica, showed a larger ultimate capacity load than the control beam. For beams in group A, the beam with 1% Nano-silica and the beam with 1.5% Nano-silica had an average increase in ultimate load capacity of 15% and 6%, respectively when they were compared with the control beams. For beams in group B, the beam with 1% Nano-silica, the beam with 1.5% Nano-silica and the beam with 2% Nano-silica had an average increase in ultimate load capacity of 17%, 13% and 10%, respectively.
- The optimum content of Nano-Silica was 1% as a replacement for cement. All results (compressive strength, steel mass loss, ultimate load capacity and load-deflection) were achieved when using the MNS81 mix.

Acknowledgments

Disclosure

This research did not receive any specific grant from funding agencies in the public, commercial or not-for-profit sectors. There is no Conflict of Interest

References

1. Broomfield, J.P., *Corrosion of steel in concrete: Understanding, Investigation and Repair*, E&FN, London, 1997: p. 1-15.
2. El-Reedy, M., *Steel-reinforced concrete structures: assessment and repair of corrosion*. 2007: CRC press.
3. Ožbolt, J., G. Balabanić, and M. Kušter, *3D Numerical modelling of steel corrosion in concrete structures*. Corrosion science, 2011. **53**(12): p. 4166-4177.
4. Gopu, G.N. and A. Sofi, *The influence of fiber RC beams under flexure on the chloride-induced corrosion*. Case Studies in Construction Materials, 2022. **17**: p. e01566.
5. Hosseini, P., et al., *Toward green revolution in concrete industry: The role of nanotechnology (A review)*. Australian Journal of Basic and Applied Sciences, 2011. **5**(12): p. 2768-2782.
6. Pacheco-Torgal, F. and S. Jalali, *Nanotechnology: Advantages and drawbacks in the field of construction and building materials*. Construction and building materials, 2011. **25**(2): p. 582-590.
7. Haruehansapong, S., T. Pulngern, and S. Chuchepsakul, *Effect of the particle size of nanosilica on the compressive strength and the optimum replacement content of cement mortar containing nano-SiO₂*. Construction and Building Materials, 2014. **50**: p. 471-477.
8. Zhang, P., et al., *Influence of nano-SiO₂ on properties of fresh and hardened high performance concrete: A state-of-the-art review*. Construction and Building Materials, 2017. **148**: p. 648-658.
9. Ismael, R., et al., *Influence of nano-SiO₂ and nano-Al₂O₃ additions on steel-to-concrete bonding*. Construction and Building Materials, 2016. **125**: p. 1080-1092.
10. Du, H., S. Du, and X. Liu, *Durability performances of concrete with nano-silica*. Construction and building materials, 2014. **73**: p. 705-712.
11. Heikal, M., S. Abd El Aleem, and W. Morsi, *Characteristics of blended cements containing nano-silica*. HBRC Journal, 2013. **9**(3): p. 243-255.
12. Prasath, S., S. SenthilSelvan, and E. Balaji, *Experimental study of nano silica and silica fume concrete column subjected to corrosion*. IJCIET, 2017. **8**(3): p. 708-719.
13. Zapata, L., et al., *Rheological performance and compressive strength of superplasticized cementitious mixtures with micro/nano-SiO₂ additions*. Construction and Building Materials, 2013. **41**: p. 708-716.
14. G, A., N. N, and S. R, *Behaviour of Reinforced Concrete Beam Containing Micro Silica and Nano Silica*. International Journal of Engineering Trends and Technology, 2017. **48**: p. 140-146.
15. AL-Maamar, H.F.N., *Shear Strength of Nanosilica Fiber Reinforced Concrete Beams*. 2016, Sudan University of Science and Technology.
16. Wang, X., et al., *Experimental comparison of galvanostatic methods for accelerated corrosion of steel bars in RC members*. J. Build. Mater, 2015. **1**: p. 204-210.
17. Andrade, C. and C. Alonso, *On-site measurements of corrosion rate of reinforcements*. Construction and building materials, 2001. **15**(2-3): p. 141-145.

18. El Maaddawy, T.A. and K.A. Soudki, *Effectiveness of impressed current technique to simulate corrosion of steel reinforcement in concrete*. Journal of materials in civil engineering, 2003. **15**(1): p. 41-47.
19. Mangat, P.S. and M.S. Elgarf, *Flexural strength of concrete beams with corroding reinforcement*. Structural Journal, 1999. **96**(1): p. 149-158.
20. Cairns, S., et al., *Smarter Choices: Assessing the Potential to Achieve Traffic Reduction Using 'Soft Measures'*. Transport Reviews - TRANSP REV, 2008. **28**: p. 593-618.
21. Türkmen, İ., *Influence of different curing conditions on the physical and mechanical properties of concretes with admixtures of silica fume and blast furnace slag*. Materials Letters, 2003. **57**(29): p. 4560-4569.